IEEE Access
Multidisciplinary | Rapid Review | Open Access Journal

Received 13 November 2022, accepted 26 November 2022, date of publication 5 December 2022,
date of current version 8 December 2022.

Digital Object Identifier 10.1109/ACCESS.2022.3226512

RESEARCH ARTICLE

Fault Feature Extraction Method of Reciprocating Compressor Valve Based on SPA-MF

YING LI, YUNJIE PAN, PENG BA, SHIHU WU, AND JIAWEN CHEN
School of Mechanical Engineering, Shenyang Ligong University, Shenyang 110159, China

Corresponding author: Ying Li (liyingnpu@126.com)

This work was supported in part by the Scientific Research Project of Liaoning Provincial Department of Education under Grant LG202031, in part by the Shenyang Ligong University's Research Support Program for High-Level Talents under Grant 1010147000819, and in part by the National Natural Science Foundation of China under Grant 51934002.

ABSTRACT Aiming at the problem that the traditional multifractal detrended fluctuation analysis (MFDFA) using the least squares method to fit the trend term is prone to overfitting and takes a long time, this paper proposes a new non-stationary signal analysis method—smoothed prior analysis multifractal (SPA-MF). Firstly, the time sequence data is adaptively decomposed by smooth prior analysis (SPA) to eliminate the local trends of sequence data at different scales, and then the multifractal analysis is performed on the detrended data obtained by the decomposition. At the same time, the sparrow search algorithm (SSA) is used to optimize the parameter of the SPA, so as to eliminate the trend item data more accurately. Through the simulation signal which composed of the BMS signal and noise signal, the feasibility of SPA-MF for feature extraction is proved. Finally, SPA-MF is applied to extract the features of the reciprocating compressor valve vibration signal, and the extracted reciprocating compressor valve features are input into support vector machine (SVM) for classification and recognition. Through the analysis of the experimental results, it can be seen that the recognition rate of the valve features obtained by the traditional MFDFA method is only 87.5%, and the recognition rate of the SPA-MF method proposed in this paper reaches 96.87%, and the time spent on feature extraction using SPA-MF is only about 36% of that of MFDFA method, which proves the SPA-MF method is a feature extraction method with high accuracy and effectiveness.

INDEX TERMS Reciprocating compressor valve, smooth prior analysis, MFDFA, SPA-MF.

I. INTRODUCTION

Reciprocating compressor is an important component equipment in industrial production, so it is of great practical significance to make it run normally. According to relevant research statistics, the valve fault accounts for about 60% of the total number of reciprocating compressor faults [1], therefore, it is necessary to analyze and study the valve fault of reciprocating compressor deeply.

Reciprocating compressor valve in the work will be affected by friction, impact and other factors, resulting in its vibration signal has strong nonlinear and non-stationary characteristics [2]. At present, wavelet analysis, empirical mode decomposition, variational mode decomposition, entropy method and multifractal method are mostly used to analyze and study nonlinear and non-stationary signals [3], [4], [5], [6], [7]. For example, Cai used wavelet threshold denoising (WTD) and ensemble empirical mode decomposition to analyze and process the vibration signal of diesel engine, and combined rule-based algorithm and BNs/BPNNs to achieve accurate detection and identification of diesel engine faults [8]. Ye used variational mode decomposition (VMD) and multiscale permutation entropy (MPE) to extract fault features of rolling bearings, and combined the PSO-SVM to realize accurate identification of rolling bearing status [9]. Cai used WTD and minimum entropy deconvolution methods to eliminate the noise in the signal, and combined complementary ensemble empirical mode decomposition method and Bayesian network to achieve accurate identification of early faults of permanent magnet synchronous motor [10].

The associate editor coordinating the review of this manuscript and approving it for publication was Baoping Cai.

The selection of wavelet bases in wavelet analysis is too complex, and there is uncertainty principle in wavelet analysis, which limits the development of wavelet analysis. EMD can decompose the signal adaptively and has a good signal-noise ratio, but EMD method is prone to modal aliasing and has endpoint effect. As an improvement of the EMD method, LMD requires significantly fewer iterations, and the problem of endpoint effect has been alleviated, but there is still the problem of endpoint effect. When the number of smoothing times increases, the LMD method is easy to cause the signal to advance or lag. VMD method has a very good theoretical basis as support, and has strong robustness, while effectively avoiding the phenomenon of mode aliasing. The disadvantage of VMD method is that it has boundary effect and is easily affected by burst signal. Among the above methods, the multifractal method can not only deeply describe the non-stationary and nonlinear characteristics of the signal, but also describe the self-similarity of the vibration signal, so as to extract the fault characteristics of the nonstationary signal more comprehensively and accurately. Multifractal method is easily affected by the trend of non-stationary signals when analyzing signals, therefore, based on multifractal method, kantelhardt Proposed the MFDFA method. In MFDFA, the detrended fluctuation analysis is used to eliminate the trend component in the signal, and then the signal is analyzed by combining the multifractal spectrum [11]. The characteristic parameters obtained by the MFDFA method can well reflect the characteristics of non-stationary signals, so the MFDFA method is widely applied in the mechanical fault diagnosis field. Lin et al. established the relationship between tool wear and multifractal parameters in milling process by using MFDFA method, and successfully realized the monitoring of tool condition by combining SVM [12]. Guo et al. used the variational modal decomposition (VMD) to decompose the electromechanical actuators(EMAs) into a number of intrinsic mode functions (IMFs), and then used MFDFA to extract the characteristic parameters of IMFs, and successfully realized the fault diagnosis of the EMSs[13].Liu et al. combined VMD and MFDFA methods to identify the valve state of reciprocating compressors, and introduced principal component analysis to refine the eigenvectors to obtain higher recognition rate [14]. On the basis of MFDFA method, many researchers have improved MFDFA for its problems. In order to solve the problem of choosing the orders of the detrending polynomial in MFDFA, Du et al. proposed an Adaptive Multifractal Detrended Fluctuation Analysis (AMF-DFA) method, which automatically eliminates the trend components in the signal based on correlation analysis, and proved the effectiveness of the AMF-DFA method through fault diagnosis [15]. Cao and Shi proposed a sliding window MFDFA method (W-MFDFA), which uses the sliding window technique to improve the selection value method of MFDFA, and applied this method to practical analysis [16]. The above methods do not fundamentally solve the shortcomings of MFDFA method itself: when the MFDFA method removes the trend term, it is assumed that the local trend of sequence signal is in the form of polynomial, so the least square method is used to fit the trend item signal [17]. However, the least square method is easy to lead to overfitting when fitting the trend term, and it takes a long time.

Based on the above problems, this paper proposes a new non-stationary signal analysis method-smoothed prior analysis multifractal (SPA-MF), first, the SPA method is used to eliminate the local trend of the sequence at different scales, and then the detrended data is analyzed by multifractal analysis. The SPA-MF method is used to establish the relationship between the multifractal spectrum parameters and the reciprocating compressor valve state. Through the analysis of the multifractal spectrum parameters, the accurate identification of the reciprocating compressor valve condition is finally achieved.

The rest part of this paper is organized as follows. The principle of SPA-MF is introduced in Section II. Section III combines the typical non-stationary self-similar sequence signal BMS signal and noise signal to build the simulation signal and prove the effectiveness of SPA-MF method. In Section IV, the actual reciprocating compressor valve signal is used to verify the effectiveness of the proposed method for fault feature extraction. The conclusions are given in Section V. Section VI discusses some limitations and shortcomings of this paper and the future work direction.

II. PRINCIPLE OF SPA-MF

A. SPA

SPA method was first proposed by Dr. Karjalainen et al, which can effectively remove the trend term of the sequence. Compared with traditional trend term adaptive decomposition methods such as wavelet analysis, EMD and VMD, SPA has the advantage of simple and efficient algorithm. Meanwhile, SPA decomposes the signal into trend term and detrend term, avoiding the influence of components selection on the results [18]. The specific principle of SPA algorithm is as follows:

The original time signal is set to $\boldsymbol{X}$, the trend term is set to $\boldsymbol{X}_t$, build the linear observation model of trend term:

$$\boldsymbol{X}_t = \boldsymbol{H}\theta + \boldsymbol{v} \tag{1}$$

where $\boldsymbol{H}$ is the observation matrix, θ is the regression parameter, and $\boldsymbol{v}$ is the observation error.

Solve the optimal solution $\hat{\theta}$ of θ according to Eq. (2), and then estimate the trend term of the original time signal according to $\hat{\boldsymbol{X}}_t = \boldsymbol{H}\hat{\theta}$.

$$\hat{\theta}_\lambda = \arg\min_{\theta} \left\{ \|\boldsymbol{H}\theta - \boldsymbol{X}\|^2 + \lambda^2 \|\boldsymbol{D}_d(\boldsymbol{H}\theta)\|^2 \right\} \tag{2}$$

where, λ is regularization parameter and $\boldsymbol{D}_d$ is the discrete expression of the d-order differential operator. We assume $\boldsymbol{X}$ has N local extreme points

$$\boldsymbol{X}_{\mathrm{e}} = [X_1, X_2, \cdots, X_N] \tag{3}$$

then the discrete forms of the first-order trend and the second-order trend of $\boldsymbol{X}_{\mathrm{e}}$ are:

$$\boldsymbol{X}_{\mathrm{e1}} = [X_2 - X_1, X_3 - X_2, \cdots, X_N - X_{N-1}] \tag{4}$$

$$\boldsymbol{X}_{e2} = [X_3 - 2X_2 + X_1, X_4 - 2X_3 + X_2, \cdots, X_N - 2X_{N-1} + X_{N-2}] \tag{5}$$

then we can deduce that the trend of any order of $\boldsymbol{D}_d$ is

$$\boldsymbol{D}_d = \begin{bmatrix} \frac{d(\boldsymbol{X}_{ed})_1}{dX_1} & \cdots & \frac{d(\boldsymbol{X}_{ed})_1}{dX_N} \\ \vdots & \cdots & \vdots \\ \frac{d(\boldsymbol{X}_{ed})_{N-d}}{dX_1} & \cdots & \frac{d(\boldsymbol{X}_{ed})_{N-d}}{dX_N} \end{bmatrix} \tag{6}$$

where $\boldsymbol{X}_{ed}$ is the discrete form of the d-order trend of $\boldsymbol{X}_e$, and then make the differential term $\boldsymbol{D}_d(\boldsymbol{H}\theta)$ tend to 0, then Eq. (2) can be expressed as

$$\hat{\theta}_\lambda = \left(\boldsymbol{H}^T\boldsymbol{H} + \lambda^2\boldsymbol{H}^T\boldsymbol{D}_d^T\boldsymbol{D}_d\boldsymbol{H}\right)^{-1}\boldsymbol{H}^T\boldsymbol{X} \tag{7}$$

Finally, we can estimate the trend term of the original time signal as

$$\hat{\boldsymbol{X}}_t = \boldsymbol{H}\hat{\theta}_\lambda. \tag{8}$$

In order to simplify the calculation of trend term, $\boldsymbol{H}$ is set as the identity matrix and set the order of $\boldsymbol{D}_d$ as 2, as shown in Eq. (9).

$$\boldsymbol{D}_2 = \begin{bmatrix} 1 & -2 & 1 & 0 & \cdots & 0 \\ 0 & 1 & -2 & 1 & \cdots & 0 \\ \vdots & \vdots & \vdots & \vdots & \vdots & \vdots \\ 0 & \cdots & 0 & 1 & -2 & 1 \end{bmatrix} \tag{9}$$

When the trend term of the original time signal is removed, the time detrend term $\boldsymbol{X}_{\text{det}}$ is obtained as

$$\hat{\boldsymbol{X}}_{\text{det}} = \boldsymbol{X} - \boldsymbol{H}\hat{\theta}_\lambda = \left[\boldsymbol{I} - \left(\boldsymbol{I} + \lambda^2\boldsymbol{D}_2^T\boldsymbol{D}_2\right)^{-1}\right]\boldsymbol{X}. \tag{10}$$

If $\boldsymbol{L} = \boldsymbol{I} - (\boldsymbol{I} + \lambda^2\boldsymbol{D}_2^T\boldsymbol{D}_2)^{-1}$, then $\hat{\boldsymbol{X}}_{\text{det}} = \boldsymbol{L}\boldsymbol{X}$. Through the above analysis, it can be known that the trend term and detrend term of the original time signal can be decomposed by selecting a reasonable regularization parameter λ.

B. SSA-SPA

According to the principle of SPA, it can be seen that the parameter λ is the only factor that affects the quality of the SPA decomposition, so it is necessary to optimize the parameter λ [19]. At present, the more commonly used parameter optimization methods are swarm intelligence optimization algorithms, such as Genetic Algorithm (GA), Particle Swarm Optimization (PSO), Ant Colony Algorithm (ACO), Sparrow Search Algorithm (SSA), etc. [20], [21], [22], [23]. In the above algorithms, the SSA method has the advantages of strong optimization ability and fast convergence speed. Therefore, this paper introduces the SSA to optimize the parameter λ of SPA. The principle of the SSA is [24]:

In the sparrow population, sparrows are divided into discoverers, scroungers and dangers. The position of sparrows can be represented in the following matrix:

$$\boldsymbol{P} = \begin{bmatrix} p_{1,1} & p_{1,2} & \cdots & p_{1,d} \\ p_{2,1} & p_{2,2} & \cdots & p_{2,d} \\ \vdots & \vdots & \vdots & \vdots \\ p_{n,1} & p_{n,2} & \vdots & p_{n,d} \end{bmatrix} \tag{11}$$

where n represents the number of sparrows and d represents the number of the parameters to be optimized. The discoverer leads the population to determine the feeding direction, and the location of the discoverer is updated as follows:

$$P_{i,j}^{t+1} = \begin{cases} P_{i,j}^t \cdot \exp\left(\frac{-i}{\delta \cdot iter_{\max}}\right) & \text{if } R_2 < ST \\ P_{i,j}^t + QL & \text{if } R_2 > ST \end{cases} \tag{12}$$

where t is the current iteration, $j = 1, 2, \ldots, d$. $P_{i,j}^{t+1}$ is the value of the j-th dimension of the i-th sparrow. $iter_{\max}$ is a constant. $\delta \in (0, 1]$ is a random number. R_2 and ST are the alarm value and the safety threshold respectively. Q is a random number. L is a matrix of $1 \times$ d for which each element inside is 1

The scrounger follows the discoverers to find food. The location of the scrounger is updated as follows:

$$P_{i,j}^{t+1} = \begin{cases} Q \cdot \exp\left(\frac{P_{worst}^t - P_{i,j}^t}{\delta \cdot iter_{\max}}\right) & \text{if } i > n/2 \\ P_m^{t+1} + \left|P_{i,j}^t - P_m^{t+1}\right| \cdot A^+ \cdot L & \text{otherwise} \end{cases} \tag{13}$$

where P_m is the optimal position occupied by the producer. P_{worst} is the current global worst location. A represents a matrix of $1 \times d$ for which each element inside is randomly assigned 1 or -1, and $A^+ = A^T(AA^T)^{-1}$.

Dangers are randomly selected individuals in a sparrow population to warn of the danger of predation. The location of the danger is updated as follows:

$$P_{i,j}^{t+1} = \begin{cases} P_{best}^t + \beta \cdot \left|P_{i,j}^t - P_{best}^t\right| & \text{if } f_i > f_g \\ P_m^{t+1} + K \cdot \left(\frac{\left|P_{i,j}^t - P_{worst}^t\right|}{(f_i - f_w) + \varsigma}\right) & \text{if } f_i = f_g \end{cases} \tag{14}$$

where P_{best} is the current global optimal location. β is a normal distribution of random numbers. $K \in [-1, 1]$ is a random number. f_i is the fitness value of the present sparrow. f_w and f_g are the current global best and worst fitness values, respectively. ς is the smallest constant.

The specific steps to optimize the parameter λ of SPA by using the SSA is as follows:

Step 1: Establish the parameter value range, the parameter λ value range in the text is set to 1 - 20;

Step 2: Initialize population parameters such as the number of iterations, the proportion of discoverers, etc.;

Step 3: Perform SPA decomposition on the input signal sequence;

Step 4: Calculate fitness values and sort;

Step 5: Update sparrow position according to Eq. (12) ∼ (14);

Step 6: Calculate the fitness value and update the sparrow position;

Step 7: Judge whether the stop conditions are met. If so, exit and output the results. Otherwise, repeat **steps 4-6**.

C. PRINCIPLE OF MFDFA

For non-stationary time series $x(i), i = 1, 2, \cdots, N$, the specific steps of MFDFA are as follows:

(1) The time signal is set to $\boldsymbol{X} = x(i), i = 1, 2, \cdots, N$, and perform dispersion analysis on $\boldsymbol{X}$, and get the sequence $\boldsymbol{Y}$ as

$$Y(j) = \sum_{k=1}^{j} \left[x(k) - x''\right] \quad j = 1, 2, \cdots, N \tag{15}$$

$$\bar{x} = \frac{1}{N} \sum_{K=1}^{N} x(k). \tag{16}$$

(2) Divide $\boldsymbol{Y}$ into $N_s = int(N/s)$ subintervals, each of length s. Since $\boldsymbol{Y}$ is not necessarily divisible by s, it is re-divided from the end of $\boldsymbol{Y}$ to get $2N_s$ subintervals.

(3) For $2N_s$ subintervals, use the least square method to obtain the trend item sequence $y_m(i)$ of each subinterval sequence, where $i = 1, 2, \cdots, s, m = 1, 2, \cdots, N_s$.

(4) Calculate $F^2(s, m)$, when $m = 1, 2, \cdots, N_s$, then

$$F^2(s, m) = \frac{1}{s} \sum_{i=1}^{s} \{Y[(m-1)s + i] - y_m(i)\}^2 \tag{17}$$

and when $m = N_{s+1}, N_{s+2}, \cdots, 2N_s$,then

$$F^2(s, m) = \frac{1}{s} \sum_{i=1}^{s} \{Y[N - (m-1)s + i] - y_m(i)\}^2 \tag{18}$$

(5) Average over $F^2(s, m)$ to obtain the q-order fluctuation function

$$F_q(s) = \left\{ \frac{1}{2N_s} \sum_{m=1}^{2N_s} \left[F^2(s, m)\right]^{\frac{q}{2}} \right\}^{\frac{1}{q}} \tag{19}$$

where q is non-zero real numbers, if $q = 0$ then

$$F_0(s) = exp\left\{ \frac{1}{4N_s} \sum_{m=1}^{4N_s} \ln\left[F^2(s, m)\right] \right\} \tag{20}$$

(6) After analyzing $F_q(s)$ and s, it can be found that $F_q(s)$ and s have a power-law relationship, that is

$$F_q(s) \propto s^{h(q)} \tag{21}$$

where $h(q)$ is called generalized Hurst exponent. When the time series has only single fractal properties, $h(q)$ is a constant. When the time series has multifractal characteristics, the relation of $h(q)$ and q is nonlinear.

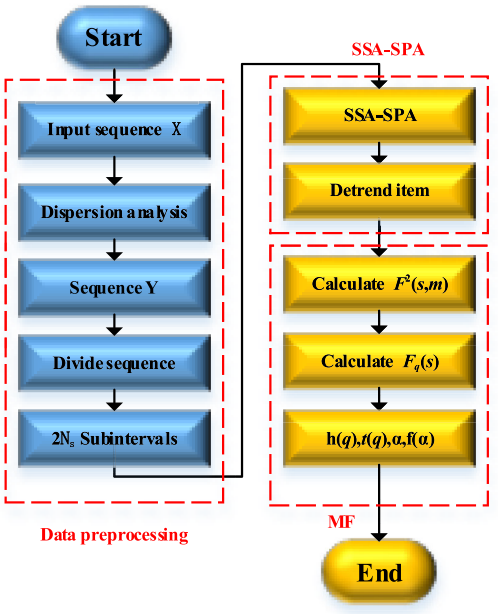

FIGURE 1. Flow chart of SPA-MF method.

(7) According to the exponent $h(q)$, the scaling exponent τ_q can be obtained, and its relationship with $h(q)$ is

$$\tau_q = qh(q) - 1 \tag{22}$$

(8) According to the Legendre transform, the multifractal singular spectral exponent α and spectral function $f(\alpha)$ can be obtained as

$$\alpha_q = d\tau_q/dq \tag{23}$$

$$f(\alpha) = q\alpha_q - \tau_q \tag{24}$$

The fractal property of time series can be judged by spectral function $f(\alpha)$. When $f(\alpha)$ is constant, time series has single fractal property. When $f(\alpha)$ is a single peak function, the time series has multifractal characteristics [25].

D. PRINCIPLE OF SPA-MF

In step (3) of Principle of MFDFA, the MFDFA method assumes that the local trend of the sequence signal is polynomial when eliminating the trend term, so the least squares method is used to fit the trend term signal. However, the least square method is easy to lead to overfitting when fitting the trend term, and it takes a long time. Therefore, this paper uses the SPA method instead of the least squares method to fit the trend term signal in the non-stationary signal, and then forms the SPA-MF method. Other steps of the SPA-MF method are the same as the MFDFA method. The flow chart of the SPA-MF method is shown in Figure 1.

III. SIMULATION ANALYSIS

In order to verify the effectiveness of the SPA-MF method, a typical non-stationary self-similar sequence BMS signal is used for simulation analysis. The time series generated by the

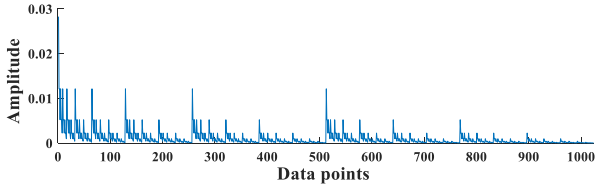

FIGURE 2. BMS simulation signal.

BMS signal is shown in Eq. (25).

$$x_i = \left(\frac{p_1}{1-p_1}\right)^{n(i-1)} (1-p_1)^{n_{max}} \quad i = 1, 2, \cdots N \tag{25}$$

In Eq. (25), both n_{max} and p_1 are parameters for generating the BMS sequence, where $p_1 \in (0, 0.5)$ and $N = 2^{n_{max}}$. Selecting $p_1 = 0.3$ and $n_{max} = 10$ to generate a BMS signal with a length of 1024 according to Reference [26], as shown in Figure 2.

The scaling exponent τ_q and order q of BMS signal have theoretical values, as shown in Eq. (26),

$$\tau_q = -\frac{\ln\left(p_1^q + p_2^q\right)}{ln2} \tag{26}$$

where $p_2 = 1 - p_1$ and $0.5 < p_2 < 1$. The generalized Hurst exponent $h(q)$ and multifractal spectrum of the BMS signal can be calculated according to Eq. (22) $\sim$ (24). Drawing the $h(q) \sim q$, $\tau_q \sim q$, and the multifractal spectrum function $f(\alpha) \sim \alpha$ of the BMS signal,as shown in Figure 3.

It can be seen from Figure 3 that $h(q)$ of the BMS signal decreases nonlinearly with q, τ_q increases nonlinearly with q, and the curves of the multifractal spectrum function $f(\alpha)$ and α show a single inverted bell shape, all indicating that the BMS signal has multifractal characteristics. The fault signal of reciprocating compressor valve has the characteristics of periodicity and randomness. In order to be closer to the actual situation, a noise signal is added on the basis of the BMS signal, and the final simulated signal is shown in Eq. (27):

$$y(i) = x(i) + a(i) \tag{27}$$

where, $x(i)$ is the BMS signal and $a(i)$ is the Periodic white noise signal. Set the parameter p_1 in BMS signal to 0.3 and 0.03 respectively to form two different time series $y_1(i)$ and $y_2(i)$.The simulation signal $y_1(i)$ is shown in Figure 4.

Use MFDFA and SPA-MF methods to solve the multifractal spectra of $y_1(i)$ and $y_2(i)$, and then extract multifractal feature parameters respectively. Figure 5 shows the multifractal spectrum and important parameter points of $y_1(i)$ under the MFDFA method. Taking Figure 5 as an example, next, several important multifractal spectrum characteristic parameters are introduced in detail.

Selecting the maximum value α_{max} of multifractal singular spectral exponent and the minimum value α_{min} of multifractal singular spectral exponent to form the characteristic parameter $\Delta\alpha$, $\Delta\alpha$ represents the width of fractal spectrum, and $\Delta\alpha$ reflects the regularity of signal fluctuation. The larger $\Delta\alpha$ is, the more irregular the signal fluctuation is, and the greater the fractal intensity of the sequence is [27];

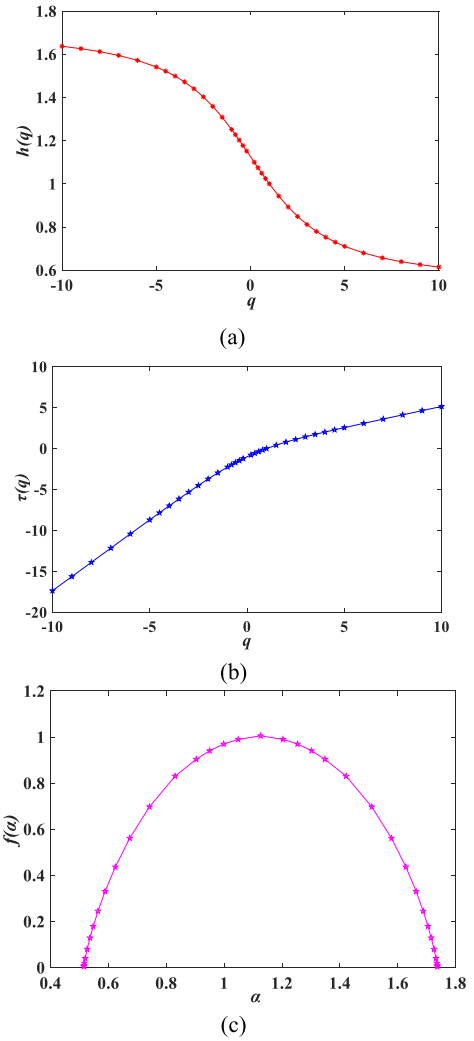

FIGURE 3. BMS signal theory results: (a) $h(q) - q$ curve of the BMS signal;(b) $\tau_q - q$ curve of the BMS signal;(c) $f(\alpha) - \alpha$ curve of the BMS signal.

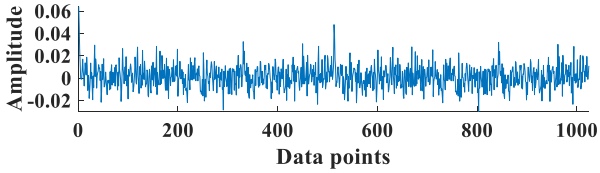

FIGURE 4. The simulation signal $y_1(i)$.

The singular spectral exponent α_0 corresponding to the maximum value $f(\alpha)$ of the singular spectral function is selected to form the characteristic parameter, α_0 reflects the nonuniformity of the signal, the smaller the α_0 is, the more irregular the signal is [28];

Using characteristic parameter $\Delta\alpha$ and characteristic parameter α_0 to form the characteristic parameter $\Delta\alpha_{dr} = (\alpha_{max} - \alpha_0)/(\alpha_0 - \alpha_{min})$.The characteristic parameter $\Delta\alpha_{dr}$ reflects the symmetry and singularity of the singular spectral function.

Selecting the singular spectral function $f(\alpha_{max})$ corresponding to the maximum value α_{max} of the singular spectral

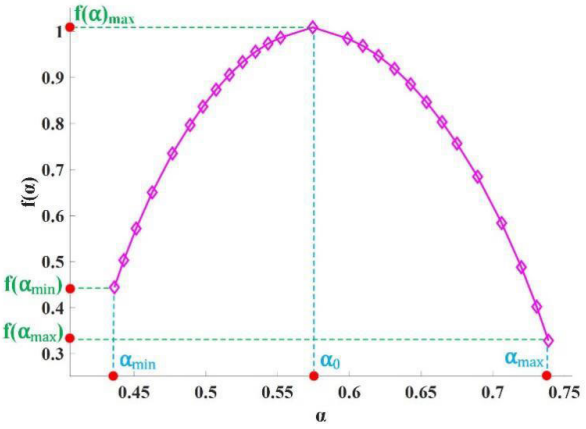

FIGURE 5. $f(\alpha) - \alpha$ curve of the $y_1(i)$.

TABLE 1. Characteristic parameters of the simulated signal based on SPA-MF and MFDFA.

	SPA-MF			MFDFA		
	Y_1	Y_2	Diff	Y_1	Y_2	Diff
$\Delta\alpha$	0.2885	0.3706	0.0821	0.3126	0.2153	0.0973
α_0	0.0568	0.0436	0.0132	0.4348	0.4831	0.0483
$\Delta\alpha_{dr}$	0.8069	1.0430	0.2361	0.4982	0.2483	0.2499
Δf	0.0200	0.3343	0.3143	0.4075	0.5382	0.1307
df	0.6173	0.7937	0.1764	0.8064	0.7054	0.101
time(s)		18			116	

exponent, and the singular spectral function $f(\alpha_{min})$ corresponding to the minimum value α_{min} of the singular spectral exponent to form the characteristic parameter $\Delta f = f(\alpha_{max}) - f(\alpha_{min})$, Δf reflects the proportion of large and small peaks in the signal. The larger the Δf is, the stronger the fractal characteristic of the sequence is;

Selecting the maximum value $f(\alpha)_{max}$ of singular spectral function and the minimum value $f(\alpha)_{min}$ of singular spectral function to form the characteristic parameter $df = f(\alpha)_{max} - f(\alpha)_{min}$ of valve, df can reflect the fractal strength of vibration signal. The larger the df is, the stronger the fractal characteristic of signal is.

Time series $y_1(i)$ and $y_2(i)$ are recorded as Y_1 and Y_2, the features extracted by MFDFA and SPA-MF are shown in Table 1.

As can be seen from Table 1, after using SPA-MF to calculate the multifractal spectral characteristic parameters of signals Y_1 and Y_2 respectively, the parameters $\Delta\alpha_{dr}$, Δf, df have obvious distinction, and the parameter $\Delta\alpha$ and α_0 have weak distinction. Using the MFDFA method to calculate the multifractal spectral characteristic parameters of the signals Y_1 and Y_2 respectively, the parameter $\Delta\alpha_{dr}$ has obvious distinction, the parameters Δf and df have small distinction, and the parameters $\Delta\alpha$ and α_0 are almost indistinguishable. Meanwhile, under the same condition, it took 116 s to extract the feature parameters using the MFDFA method, while only 16 s using the SPA-MF method. To sum up, for simulation signals Y_1 and Y_2, compared with the traditional MFDFA method, the SPA-MF method proposed in this paper can extract the multifractal spectrum features of simulation signals faster, and the multifractal spectrum features extracted by SPA-MF method can more clearly distinguish two different signals, which proves the feasibility of extracting signal features by SPA-MF method.

FIGURE 6. Reciprocating compressor experimental platform.

IV. EXPERIMENT

A. SPECIFIC STEPS

Step 1: Using the 2D12-70/0.1-13 reciprocating compressor build a signal acquisition system to collect separately the valve vibration acceleration signals under the normal state, valve plate fracture state, valve plate gap state, and valve spring failure state.

Step 2: Calculating the generalized Hurst exponent $h(q)$, the scaling exponent τ_q, and the multifractal spectrum of the valve vibration acceleration signal data in different states by the SPA-MF method proposed in this paper.

Step 3: Calculating the eigenvectors group $F = [\Delta\alpha, \alpha_0, \Delta\alpha_{dr}, \Delta f, df]$ of the valve faults by the multifractal spectrum, and inputting the eigenvectors and corresponding labels into the SVM for training and testing, and finally comparing the test results with the traditional MFDFA method.

B. EXPERIMENT

The research object of this paper is 2D12-70/0.1-13 reciprocating compressor, the discharge capacity is 70 m^3/min, the discharge pressures of I stage and II stage are 0.2746-0.2942 Mpa and 1.2749 Mpa respectively, and the crankshaft speed is 496 r/ min. The acceleration sensor is used to collect the vibration signals of the normal state and three fault states of the suction valve position of the secondary cylinder, the measuring point of the acceleration sensor is set on the valve cover, the sampling frequency is set to 50 kHz, and the sampling time is 4 s [29]. The reciprocating compressor is shown in Figure 6.

Figure 7 shows the picture of the valve in different states, the upper left of the picture shows the normal state, the lower left of the picture shows the valve plate fracture state, the upper right of the picture shows the valve plate gap state, and the lower right of the picture shows the valve spring failure

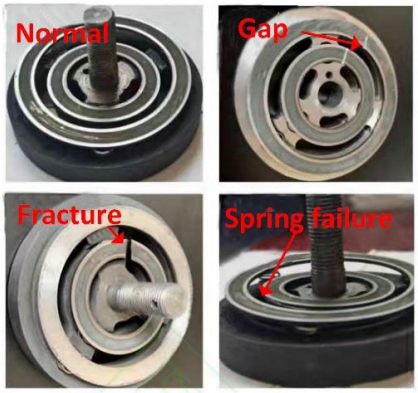

FIGURE 7. Picture of valve in different states.

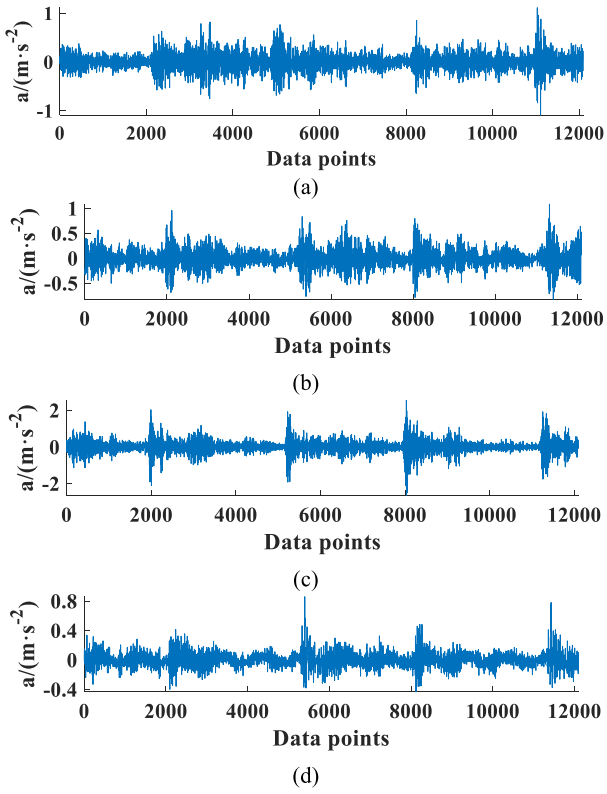

FIGURE 8. Vibration signal of reciprocating compressor valve under four states:(a) Normal state; (b) Valve plate fracture state; (c) Valve plate gap state; (d) Valve spring failure state.

state. Normally, the valve has six springs. When the valve is in the valve spring failure state, the valve has four springs.

Taking 40 groups of samples in each of the four states of the reciprocating compressor valve, a total of 160 groups, with 12096 points in each group. The vibration acceleration signals of the reciprocating compressor valve under four states are shown in Figure 8.

In order to verify that the SPA method can effectively decompose the trend item and detrend item of vibration signal, take the valve spring failure state as an example, the vibration acceleration signal of the valve is decomposed by SPA. After optimizing SPA parameter by SSA method, when

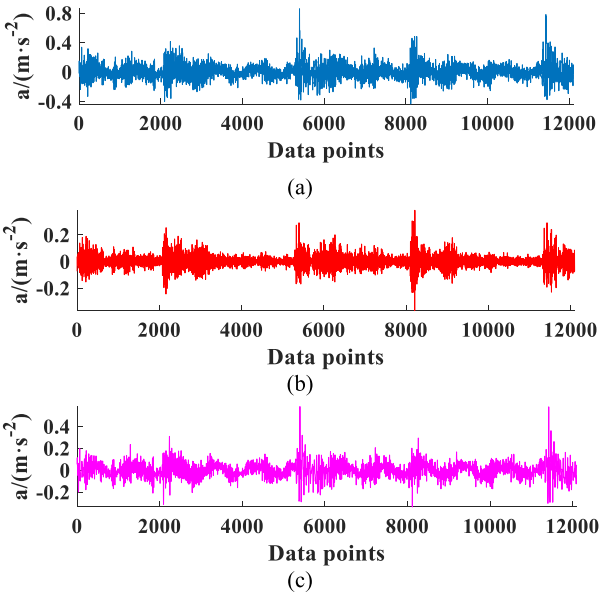

FIGURE 9. SPA decomposition result of vibration signal of the valve spring failure state:(a) Original signal; (b)Detrended item signal; (c)Trended item signal.

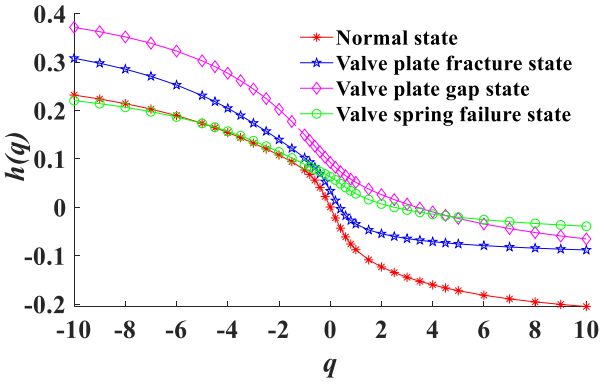

FIGURE 10. $h(q) - q$ curve of valve under four states.

$\lambda = 6$, the SPA has the best decomposition effect. The decomposition results are shown in Figure 9.

According to Figure 9, it can be seen that after the signal is decomposed by SPA, the decomposed trend item and detrend item are clearly distinguished, and the detrend item effectively retains the vibration characteristics of the original vibration signal.

The SPA-MF method is used to analyze the vibration acceleration signal data under the four states of the valve, and the corresponding relationship between the generalized Hurst exponent $h(q)$ and q under the four states of the valve is obtained, as shown in Figure 10

It can be seen from Figure 10 that the generalized Hurst exponents $h(q)$ and q of the reciprocating compressor valve signal have a nonlinear relationship, which indicating that the valve vibration signal has multifractal characteristics. With the increase of q, $h(q)$ gradually decreases. When $q < 0$, the $h(q)$ values of the vibration signal under the normal state and the valve spring failure state are similar, and have clear distinction with the other two states. When $q < 0$, the $h(q)$

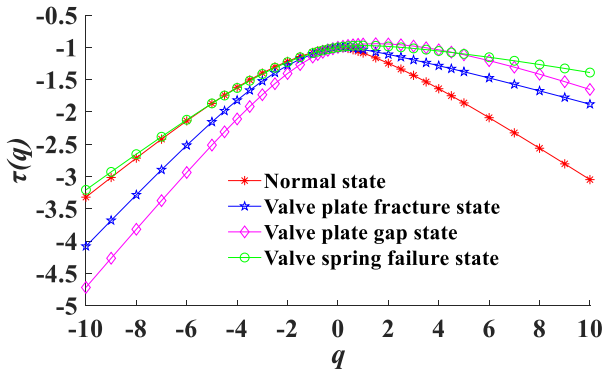

FIGURE 11. $\tau q - q$ curve of valve under four states.

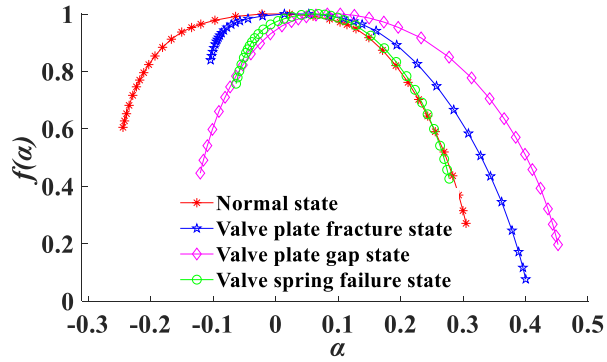

FIGURE 12. $f(\alpha) - \alpha$ curve of valve under four states.

value of the vibration signal under the valve plate gap state is the largest, and the $h(q)$ values under the valve spring failure state and the normal state are smaller; near $q = 0$, $h(q)$ changes the fastest; when $q > 0$, the $h(q)$ value in the normal state is significantly smaller than the value of the other three states of the valve.

In order to analyze the multifractal characteristics of the four states of the valve more deeply, the corresponding relationship between the scaling exponent τ_q and q under the four states of the valve is drawn, as shown in Figure 11.

It can be seen from Figure 11 that with the increase of q, the scaling exponent τ_q of the valve signal changes in an upward convex shape. When $q < 0$, the τ_q value increases nonlinearly with q, in which the τ_q value under the valve plate gap state is the smallest, and the τ_q values under the normal state and the valve spring failure state are similar and larger than the other two states; when $q = 0$, $\tau_q = -1$; when $q > 0$, τ_q decreases nonlinearly with q, and the τ_q value in the normal state decreases rapidly, which is significantly smaller than the τ_q value in the other three states of the valve.

According to the generalized Hurst exponent $h(q)$ and the scaling exponent τ_q, draw the multifractal spectrum under the four states of the valve, as shown in Figure 12.

As can be seen from Figure 12, the multifractal spectrum of the four states of the valve presents an inverted bell shape, indicating that the vibration signal of the valve has multifractal characteristics. Among them, the figure of the valve in the valve spring failure state is significantly narrower than that in other three states, and the multifractal spectrum in the normal state changes slowly.

TABLE 2. Characteristic parameter values of the valve under four states.

	$\Delta\alpha$	α_0	$\Delta\alpha_{dr}$	Δf	df
Normal	0.5491	0.0224	1.0589	-0.3343	0.7289
Fracture	0.5045	0.0532	2.2079	-0.7629	0.9234
Gap	0.5728	0.1035	1.5557	-0.2491	0.8033
Spring failure	0.3413	0.0688	1.5845	-0.3308	0.5735

According to the analysis of the above simulation signal, the multifractal spectrum parameters $\Delta\alpha, \alpha_0, \Delta\alpha_{dr}, \Delta f, df$ of the valve are extracted to form the feature vector $F = [\Delta\alpha, \alpha_0, \Delta\alpha_{dr}, \Delta f, df]$ of the valve. The characteristic parameter values of valve under four states are shown in Table 2.

It can be seen from Table 2 that the fractal spectrum width ($\Delta\alpha$) of the normal state and the valve plate gap state is larger than the other two states, and the fractal spectrum width of the valve spring failure state is the smallest; The parameter α_0 can reflect the nonuniformity of the signal. It can be seen that the parameter α_0 in the normal state is smaller, that is, the nonuniformity in the normal state is small, and the nonuniformity in the other three states are larger, which is also in line with the actual situation; $\Delta\alpha_{dr}$ reflects the symmetry and singularity of the singular spectral function, it can be seen from Table 2 that the characteristic value $\Delta\alpha_{dr}$ under the valve plate fracture state is relatively large, and the characteristic value $\Delta\alpha_{dr}$ under the normal state is the smallest. It can be seen from Table 2 that the parameter Δf under the valve plate fracture state is small and is clearly distinguished from the other three states; It can be seen from the parameter df that the value of df under the valve plate fracture state is the largest, indicating that the fractal strength is the largest, while the value of df under the valve spring failure state is the smallest, indicating that the fractal strength reflected by the parameter df is the smallest.

Based on the analysis of the five parameters in the four states of the valve, it can be seen that a single characteristic parameter cannot completely distinguish the working state of the valve, so the five characteristic parameters are combined to form the characteristic vector of the valve: $F = [\Delta\alpha, \alpha_0, \Delta\alpha_{dr}, \Delta f, df]$. Corresponding labels are set for the four states of the reciprocating compressor valve, in which label 1 corresponds to the normal state, label 2 corresponds to the valve plate fracture state, label 3 corresponds to the valve plate gap state, and label 4 corresponds to the valve spring failure state. 32 of the 40 groups of data in each of the four states are selected as the training set (80%), and 8 groups are selected as the test set (20%) to verify the effectiveness of the fault feature extraction method. Figure 13 shows the SVM diagnosis results based on the SPA-MF method and the MFDFA method respectively, and the SVM diagnosis results based on the SPA-MF method and the MFDFA method are listed in Table 3 for comparative analysis.

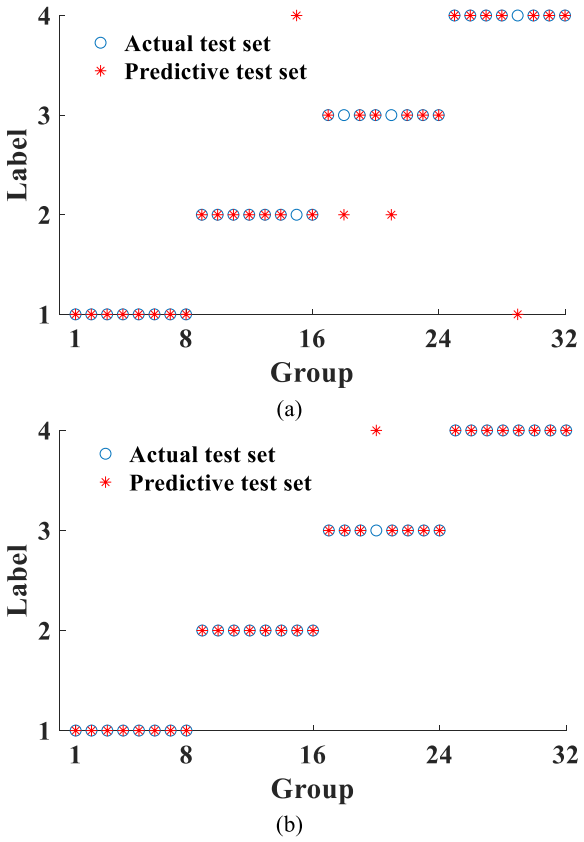

FIGURE 13. SVM diagnosis results based on SPA-MF and MFDFA respectively:(a) SVM diagnosis results based on MFDFA; (b) SVM diagnosis results based on SPA-MF.

TABLE 3. Comparison results.

	MFDFA	SPA-MF
Normal	100%	100%
Fracture	87.5%	100%
Gap	75%	87.5%
Spring failure	87.5%	100%
Total	87.5%	96.87%
Time (s)	1016	366

It can be seen from Figure 13 that when the MFDFA method is used, except for the normal state, multiple groups of data are incorrectly identified in other states. When the SPA-MF method is used, only a group of data in the valve plate gap state is incorrectly identified as other states, which indicates that the SPA-MF method has better recognition rate. For the error recognition of the state, the main reason is that the noise factor has not been completely eliminated in the signal decomposition process. In addition, the number of samples will also affect the training effect of SVM, resulting in the error recognition of the valve state. As can be seen from Table 3, under the same conditions, the total recognition rate of the valve features extracted by the traditional MFDFA method is only 87.5%, and the total recognition rate of the SPA-MF method proposed in this paper reaches 96.87%. Meanwhile, it takes an average of 1016 s to extract the characteristic parameters of the reciprocating compressor by using the MFDFA method, while it only takes an average of 366 s to extract the characteristic parameters by using the SPA-MF method, and the time used is only about 36% of the MFDFA method, which proves the accuracy and efficiency of SPA-MF method in the valve feature extraction.

V. CONCLUSION

The fault feature extraction method based on SPA-MF proposed in this paper can draw the following conclusions after experimental research and analysis.

(1) Aiming at the problem that the traditional MFDFA method using the least squares method to fit the trend term is easy to lead to overfitting and takes a long time, this paper proposes a new non-stationary signal analysis method - SPA-MF, on the basis of solving the above problems, the method further plays the role of denoising, at the same time, the feasibility of the SPA-MF method is proved by the simulation signal.

(2) The characteristic vector of the reciprocating compressor valve composed of the parameters of the multifractal spectrum obtained by the SPA-MF method can comprehensively and quantitatively reflect the characteristics of the valve vibration signal, so as to extract effectively the signal characteristics of the reciprocating compressor valve under different states.

(3) Compared with the MFDFA method, the SPA-MF method can extract the fault characteristics of the reciprocating compressor valve faster, and can more accurately distinguish the vibration fault characteristics of different states of valve.

VI. FUTURE WORK

This paper proposes a new non-stationary signal analysis method, which successfully realizes the feature extraction and state recognition of the reciprocating compressor valve. The SPA-MF method is not only suitable for fault diagnosis of reciprocating compressor in the future, but also suitable for fault diagnosis of other mechanical equipment, so it has great application prospects. However, this paper still has some limitations and shortcomings, mainly including two aspects: (1) When studying the valve fault, the composite failure of valve is not studied. (2) This paper does not study the problem of fault characteristics under different speeds and loads. Next, we will conduct a more in-depth study on the above issues.

REFERENCES

[1] Y. Zhang, J. Ji, and B. Ma, "Fault diagnosis of reciprocating compressor using a novel ensemble empirical mode decomposition-convolutional deep belief network," *Measurement*, vol. 156, May 2020, Art. no. 107619.
[2] G.-J. Chen, L.-Q. Zou, H.-Y. Zhao, and Y.-Q. Li, "An improved local mean decomposition method and its application for fault diagnosis of reciprocating compressor," *J. Vibroeng.*, vol. 18, no. 3, pp. 1474–1485, May 2016.
[3] Z. Liu, L. Zhang, and J. Carrasco, "Vibration analysis for large-scale wind turbine blade bearing fault detection with an empirical wavelet thresholding method," *Renew. Energy*, vol. 146, pp. 99–110, Feb. 2020.
[4] X. Ye, Y. Hu, J. Shen, R. Feng, and G. Zhai, "An improved empirical mode decomposition based on adaptive weighted rational quartic spline for rolling bearing fault diagnosis," *IEEE Access*, vol. 8, pp. 123813–123827, 2020.

[5] W. Ying, J. Tong, Z. Dong, H. Pan, Q. Liu, and J. Zheng, "Composite multivariate multi-scale permutation entropy and Laplacian score based fault diagnosis of rolling bearing," *Entropy*, vol. 24, no. 2, p. 160, Jan. 2022.
[6] D. Yang, Y. Lv, R. Yuan, H. Li, and W. Zhu, "Robust fault diagnosis of rolling bearings via entropy-weighted nuisance attribute projection and neural network under various operating conditions," *Structural Health Monitor.*, vol. 21, no. 6, pp. 2890–2909, Nov. 2022.
[7] J. Li, Y. Cao, Y. Ying, and S. Li, "A rolling element bearing fault diagnosis approach based on multifractal theory and gray relation theory," *PLoS ONE*, vol. 11, no. 12, Dec. 2016, Art. no. e0167587.
[8] B. Cai, X. Sun, J. Wang, C. Yang, Z. Wang, and X. Kong, "Fault detection and diagnostic method of diesel engine by combining rule-based algorithm and BNs/BPNNs," *J. Manuf. Syst.*, vol. 57, pp. 148–157, Oct. 2020.
[9] M. Ye, X. Yan, and M. Jia, "Rolling bearing fault diagnosis based on VMD-MPE and PSO-SVM," *Entropy*, vol. 23, no. 6, p. 762, Jun. 2021.
[10] B. Cai, K. Hao, Z. Wang, C. Yang, X. Kong, Z. Liu, R. Ji, and Y. Liu, "Data-driven early fault diagnostic methodology of permanent magnet synchronous motor," *Exp. Syst. Appl.*, vol. 177, Sep. 2021, Art. no. 115000.
[11] J. W. Kantelhardt, S. A. Zschiegner, E. Koscielny-Bunde, S. Havlin, A. Bunde, and H. E. Stanley, "Multifractal detrended fluctuation analysis of nonstationary time series," *Phys. A, Stat. Mech. Appl.*, vol. 316, pp. 87–114, Dec. 2002.
[12] J. Lin, C. Dou, and Q. Wang, "Comparisons of MFDFA, EMD and WT by neural network, Mahalanobis distance and SVM in fault diagnosis of gearboxes," *Sound Vibrat.*, vol. 516, no. 2, pp. 12–16, 2018.
[13] J. Guo, A. Li, and R. Zhang, "Tool condition monitoring in milling process using multifractal detrended fluctuation analysis and support vector machine," *Int. J. Adv. Manuf. Technol.*, vol. 110, nos. 5–6, pp. 1445–1456, Sep. 2020.
[14] Y. Liu, J. Wang, Y. Li, H. Zhao, and S. Chen, "Feature extraction method based on VMD and MFDFA for fault diagnosis of reciprocating compressor valve," *J. Vibroeng.*, vol. 19, no. 8, pp. 6007–6020, Dec. 2017.
[15] W. Du, M. Kang, and M. Pecht, "Fault diagnosis using adaptive multifractal detrended fluctuation analysis," *IEEE Trans. Ind. Electron.*, vol. 67, no. 3, pp. 2272–2282, Mar. 2020.
[16] G. X. Cao and A. N. Shi, "Multifractal analysis of Shanghai stock market returns application of sliding window MFDFA method," *Math. Statist. Manage.*, vol. 26, no. 5, pp. 875–880, 2007.
[17] H. Liu, J. Jing, and J. Ma, "Fault diagnosis of electromechanical actuator based on VMD multifractal detrended fluctuation analysis and PNN," *Complexity*, vol. 2018, pp. 1–11, Aug. 2018.
[18] P. A. Karjalainen, "Regularization and Bayesian methods for evoked potential esimation," Ph.D. thesis, Dept. Appl. Phys., Univ. Kuopio, Kuopio, Finland, 1997. [Online]. Available: http://venda.uku.fi/research/biosignal/publications/
[19] S. Dai, Q. Chen, H. Dai, and Z. Nie, "Rolling bearing fault diagnosis based on smoothness priors approach and fuzzy entropy," *J. Aerosp. Power*, vol. 34, no. 10, pp. 2218–2226, 2019.
[20] R. Shi, B. Wang, Z. Wang, J. Liu, X. Feng, and L. Dong, "Research on fault diagnosis of rolling bearings based on variational mode decomposition improved by the niche genetic algorithm," *Entropy*, vol. 24, no. 6, p. 825, Jun. 2022.
[21] K. Zhang, J. Su, S. Sun, Z. Liu, J. Wang, M. Du, Z. Liu, and Q. Qiang, "Compressor fault diagnosis system based on PCA-PSO-LSSVM algorithm," *Sci. Prog.*, vol. 104, no. 3, 2021, Art. no. 368504211026110.
[22] S. H. Bai, L. R. Guang, and Z. W. Liu, "Applied research of ant colony algorithm in fault diagnosis," *Adv. Mater. Res.*, vol. 1037, pp. 353–356, Oct. 2014.
[23] J. Lv, W. Sun, H. Wang, and F. Zhang, "Coordinated approach fusing RCMDE and sparrow search algorithm-based SVM for fault diagnosis of rolling bearings," *Sensors*, vol. 21, no. 16, p. 5297, Aug. 2021.
[24] J. Xue and B. Shen, "A novel swarm intelligence optimization approach: Sparrow search algorithm," *Syst. Sci. Control Eng.*, vol. 8, no. 1, pp. 22–34, Jan. 2020.
[25] Q. Xiong, W. Zhang, Y. Xu, Y. Peng, and P. Deng, "Alpha-stable distribution and multifractal detrended fluctuation analysis-based fault diagnosis method application for axle box bearings," *Shock Vibrat.*, vol. 2018, pp. 1–12, Nov. 2018.
[26] X. Zhang, J. Zhao, X. Zhang, X. Ni, H. Li, and F. Sun, "A novel hybrid compound fault pattern identification method for gearbox based on NIC, MFDFA and WOASVM," *J. Mech. Sci. Technol.*, vol. 33, no. 3, pp. 1097–1113, Mar. 2019.
[27] X. Liang, Y. Luo, F. Deng, and Y. Li, "Application of improved MFDFA and D-S evidence theory in fault diagnosis," *Appl. Sci.*, vol. 12, no. 10, p. 4976, May 2022.
[28] X. Liang, Y. Luo, F. Deng, and Y. Li, "Investigation on vibration signal characteristics in a centrifugal pump using EMD-LS-MFDFA," *Processes*, vol. 10, no. 6, p. 1169, Jun. 2022.
[29] H. Zhao, J. Wang, H. Han, and Y. Gao, "A feature extraction method based on HLMD and MFE for bearing clearance fault of reciprocating compressor," *Measurement*, vol. 89, pp. 34–43, Jul. 2016.

YING LI was born in China, in 1986. She received the Ph.D. degree in chemical process machinery from Northeast Petroleum University, China. She is currently a Lecturer at the School of Mechanical Engineering, Shenyang Ligong University. Her research interests include mechanical equipment condition monitoring and fault diagnosis.

YUNJIE PAN was born in China, in 1998. He received the B.S. degree from the School of Mechanical Engineering, Shenyang Ligong University, Shenyang, China, in 2020, where he is currently pursuing the M.S. degree with the School of Mechanical Engineering. His research interest includes fault diagnosis of mechanical equipment.

PENG BA was born in China, in 1963. He received the M.S. degree from the Shenyang University of Technology, Shenyang, China. He is currently a Professor at the School of Mechanical Engineering, Shenyang Ligong University. His research interests include reciprocating compressor technology development and application.

SHIHU WU was born in China, in 1998. He received the B.S. degree from the School of Mechanical Engineering, Jingchu University of Technology, Jingmen, China, in 2021. He is currently pursuing the M.S. degree with the School of Mechanical Engineering, Shenyang Ligong University, Shenyang. His research interest includes fault diagnosis of mechanical equipment.

JIAWEN CHEN was born in China, in 1998. He received the Junior College degree from the School of Mechanical and Vehicle Engineering, Linyi University, Linyi, China, in 2019, and the B.S. degree from the School of Mechanical Engineering, Linyi University, in 2021. He is currently pursuing the M.S. degree with the School of Mechanical Engineering, Shenyang Ligong University, Shenyang. His research interest includes fault diagnosis of mechanical equipment.